DALTON

Tuning the nature of the exchange interaction in out-of-plane oximato-bridged dinuclear copper(II) complexes

Beatriz Cervera,[a] Rafael Ruiz,[a] Francesc Lloret,[a] Miguel Julve,*[,a] Juan Cano,[a] Juan Faus,[a] Claudette Bois[b] and Jerzy Mrozinski[c]

[a] *Departament de Química Inorgànica, Facultat de Química de la Universitat de València, Dr. Moliner 50, 46100-Burjassot (València), Spain*
[b] *Laboratoire de Chimie des Métaux de Transition, URA 419 CNRS, Université Pierre et Marie Curie, 75252 Paris, France*
[c] *Faculty of Chemistry, University of Wroclaw, 50383 Wroclaw, Poland*

The dinuclear copper(II) complexes of formula $[\{Cu(Hdmg)_2\}_2]$ **1**, $[\{Cu(Hbdmg)\}_2][ClO_4]_2$ **2**, $[\{Cu(Hdeg)_2\}_2]$ **3** and $[\{Cu(Hchd)_2\}_2]$ **4** (H_2dmg, H_2bdmg, H_2deg and H_2chd = dimethylglyoxime, 3,10-dimethyl-4,9-diazadodeca-3,9-diene-2,11-dione dioxime, diethylglyoxime and cyclohexane-1,2-dione dioxime) have been synthesized. The structures of **3** and **4** have been determined by single-crystal X-ray diffraction methods. Both consist of centrosymmetric dinuclear bis(alkyl)glyoximatocopper(II) entities where the units are staggered so that the copper atom of one unit is directly opposite to the oxime-oxygen atom of the other, as previously found for **1** and **2**. Each metal atom in **3** and **4** is five-co-ordinate with four imine-nitrogen atoms comprising the basal plane and an oximate-oxygen atom in the apical position. The copper–imine nitrogen bond lengths (average 1.957 and 1.953 Å in **3** and **4**, respectively) are shorter than that of the axial copper–oximate oxygen [2.263(3) (**3**) and 2.242(3) Å (**4**)]. An oxime proton is lost from the ligand in the complex formation, the remaining oxime proton being involved in a hydrogen bond between the peripheral oxime oxygens of the same bis(alkyl)glyoximatocopper(II) unit. The intramolecular copper–copper separation is 3.898(1) (**3**) and 3.825(1) Å (**4**). Variable-temperature magnetic susceptibility measurements showed the occurrence of intramolecular ferro- (**1**, **3** and **4**) and antiferro-magnetic exchange interactions (**2**), the singlet–triplet energy gap J being +9.1 (**1**), −1.9 (**2**), +1.0 (**3**) and +3.1 cm^{-1} (**4**). The analysis of the exchange pathway through the out-of-plane oximato bond in this family has been substantiated by extended-Hückel calculations and a quasi-linear correlation between the value of J and the angle at the Cu–O–N (α) has been found. The influence of the size of the imine-carbon alkyl substituents on both the nature and magnitude of J is discussed in the light of the available structural information.

The in-plane oximato bridge exhibits a remarkable ability to transmit strong antiferromagnetic interactions between paramagnetic centres which are separated by more than 3.5 Å. So, the singlet–triplet energy gap J in bis(oximato)-bridged copper(II) dinuclear complexes can be as large as -1000 cm^{-1}, these compounds being almost diamagnetic even at room temperature.[1–4] The large overlap between the two d_{xy}-type magnetic orbitals of the metal atoms through the diatomic oximato bridge (see Scheme 1) accounts for such a strong magnetic coupling. The values of J of dimeric copper(II) complexes involving other efficient well known bridging systems such as oxalato,[5] oxamidato,[6] dithiooxamidato[7] and tetrathiooxalato[8] although large are smaller. The strong magnetic coupling which can be achieved through the oximato bridge together with the possibility of using mononuclear oximato-containing metal complexes as precursors of di-,[2–4,9] tri-,[9a,10] tetra-nuclear[11] and chain[12] homo- and hetero-polymetallic compounds have attracted the attention of magnetochemists in the last five years. The nuclearity tailoring in these systems is achieved through the reaction of very stable mononuclear oximato-containing complexes such as [M(Hpdmg)] (**a**) and $[M(Hdmg)_2]$ (**b**) (H_2pdmg = 3,9-dimethyl-4,8-diazaundeca-3,8-diene-2,10-dione dioxime, H_2dmg = dimethylglyoxime and M = divalent metal ion) with metal ions previously co-ordinated to suitable blocking ligands. In the absence of outer ligands, the reaction of $[Cu(dmg)_2]^{2-}$-type complexes with metal ions yields chain compounds exhibiting metamagnetic behaviour,[12a] and bulk ferro- and antiferromagnetic ordering.[12b] Another very interesting aspect of the chemistry of the oximato-containing copper(II) complexes is the easy dimerization through out-of-plane oxime to metal bonds. The two crystallographically characterized examples

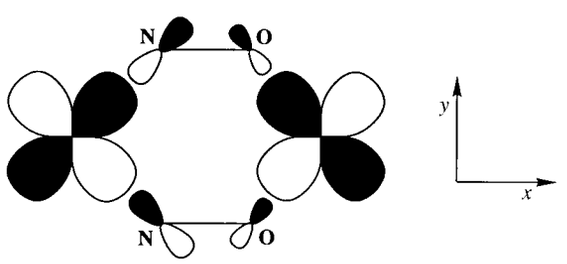

Scheme 1

are $[\{Cu(Hdmg)_2\}_2]$ **1**[13] and $[\{Cu(Hbdmg)\}_2][ClO_4]_2$ **2**[14] (**a**) (H_2-bdmg = 3,10-dimethyl-4,9-diazadodeca-3,9-diene-2,11-dione dioxime).

The present contribution is devoted to an analysis of the exchange coupling through the out-of-plane oxime to metal bonds in this family of dimeric copper(II) complexes. We have prepared and structurally characterized the two related dinuclear compounds $[\{Cu(Hdeg)_2\}_2]$ **3** (**b**) and $[\{Cu(Hchd)_2\}_2]$ **4** (**c**) (H_2deg = diethylglyoxime and H_2chd = cyclohexane-1,2-dione dioxime). The structures of **3** and **4**, the investigation of the magnetic properties of **1**–**4** and the corresponding magneto-structural correlation for this family of copper(II) compounds are presented herein.

Experimental

Materials

The complexes **1**, **2** and copper(II) hydroxide were prepared as reported in the literature.[13a,14–16] Copper(II) perchlorate hexa-

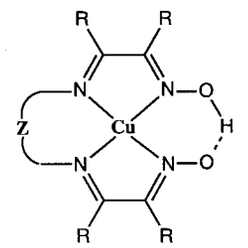

R = Me , Z = Pr ; [Cu(Hpdmg)]$^+$

R = Me , Z = Bu ; [Cu(Hbdmg)]$^+$

a

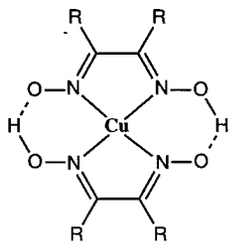

R =Me ; [Cu(Hdmg)$_2$]

R =Et ; [Cu(Hdeg)$_2$]

R =Ph ; [Cu(Hdpg)$_2$]

b

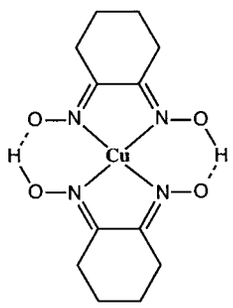

[Cu(chd)$_2$]

c

hydrate, potassium hydroxide, H_2chd, $NH_2OH·HCl$, 1,4-diaminobutane, butane-2,3-dione monoxime and hexane-3,4-dione were from commercial sources and used as received. Elemental analyses (C, H, N) were performed by the Microanalytical Service of the Universidad Autónoma de Madrid (Spain). Copper contents were determined by atomic absorption spectrometry.

Preparations of pro-ligands and complexes

H_2deg. This preparation followed the general method used for other *vic*-dioximes: a methanolic solution of potassium hydroxide (50 mmol, 20 cm^3) was added dropwise to an ice-chilled methanolic solution of $NH_2OH·HCl$ (50 mmol, 50 cm^3). The white precipitate of potassium chloride was filtered off and hexane-3,4-dione (25 mmol) was added dropwise to the remaining solution under continuous stirring. The yellow solution was kept in a freezer for 1 d and the white solid formed was filtered off and washed with cold methanol and diethyl ether. Yield *ca*. 80% (Found: C, 49.8; H, 8.7; N, 19.8. Calc. for $C_6H_{12}N_2O_2$: C, 50.0; H, 8.35; N, 19.45%). The most relevant IR features of H_2deg are a strong and broad absorption with two peaks at 3240 and 3210 cm^{-1}, [ν(OH) stretch], a medium-intensity peak at 1680 cm^{-1} and a weak absorption at 1620 cm^{-1} [ν(CC) and ν(CN) stretching vibrations], and two strong and sharp peaks at 1060 and 980 cm^{-1} [ν(NO) stretching vibrations].[17]

[{Cu(Hdeg)$_2$}$_2$] 3. Freshly made copper(II) hydroxide (5 mmol) was added to a hot methanolic solution of H_2deg (10 mmol, 50 cm^3). The resulting black-brown solution was refluxed for 0.5 h. Complex **3** was obtained as red needles from the filtered solution by slow evaporation at room temperature. Yield *ca*. 75% (Found: C, 41.45; H, 6.95; Cu, 18.0; N, 16.5. Calc. for $C_{24}H_{44}Cu_2N_8O_8$: C, 41.2; H, 6.3; Cu, 18.2; N, 16.0%).

[{Cu(Hchd)$_2$}$_2$] 4. The synthetic procedure is similar to that for complex **3** but using H_2chd as pro-ligand. Black needles. Yield *ca*. 70% (Found: C, 41.7; H, 5.55; Cu, 18.2; N, 16.45. Calc. for $C_{24}H_{36}Cu_2N_8O_8$: C, 41.65; H, 5.55; Cu, 18.35; N, 16.45%).

The IR spectra of complexes **2**–**4** have in common the occurrence of a broad absorption at *ca*. 2600 cm^{-1}, a weak peak at 1660 (**2**), 1640 (**3**) and 1635 cm^{-1} (**4**), and a sharp medium-intensity peak at 836 (**2**), 860 (**3**) and 833 cm^{-1} (**4**). Corresponding absorptions were observed in the spectrum of **1** at 2600, 1728 and 860 cm^{-1} and were assigned to ν(OH) stretching, δ(OH) bending and γ(OH) (out-of-plane) deformation modes of the hydrogen-bonded O–H · · · O group, respectively.[17,18] The strong absorption observed at 1515 (**2**), 1531 (**3**) and 1526 cm^{-1} (**4**) may be assigned to the ν(CN) stretching vibration, whereas the strong peaks at 1195, 1110 and 1060 cm^{-1} (**3**) and 1205 and 1060 cm^{-1} (**4**) could be attributed to the ν(NO) stretching modes. The strong and broad absorption of the perchlorate at *ca*. 1100 cm^{-1} for complex **2** obscures the region of the NO stretching modes and precludes their observation. These spectral features are consistent with the occurrence of both O–H · · · O interactions and oxime to metal bonds in **1**–**4** in full agreement with the structural information.

Physical techniques

The infrared spectra of complexes **1**–**4** were recorded on a Perkin-Elmer 1750 FTIR spectrophotometer as KBr pellets in the 4000–300 cm^{-1} region. The magnetic susceptibility measurements were carried out on polycrystalline samples in the temperature range 4.2–290 K with a fully automatized AZTEC DSM8 pendulum-type susceptometer[19] (**1**, **3** and **4**) equipped with a TBT continuous-flow cryostat and a Brüker BE15 electromagnet operating at 1.3 T, and with a sensitive Sartorius M-25D device (Faraday method) (**2**) equipped with an Oxford Instruments CF-1200 continuous-flow cryostat and an electromagnet operating at 5.25 T. The apparatus were calibrated with Hg[Co(NCS)$_4$]. Diamagnetic corrections were estimated from Pascal's constants[20] as -242×10^{-6} (**1**), -354×10^{-6} (**2**), -337×10^{-6} (**3**) and -364×10^{-6} cm^3 mol^{-1} (**4**). Second-order paramagnetic contributions were also considered [$N_\alpha = 60 \times 10^{-6}$ cm^3 mol^{-1} per copper(II) ion].

Crystallography

Crystals of dimensions 0.50 × 0.30 × 0.40 (complex **3**) and 0.55 × 0.40 × 0.35 mm (**4**) were mounted on Philips PW 1100 (**3**) and Enraf-Nonius CAD4 (**4**) four-circle diffractometers and used for data collection. Intensity data were collected at 18 °C by using graphite-monochromated Mo-Kα radiation (λ = 0.710 73 Å) with the ω–2θ scan method. The scan width was (0.8 + 0.34 tan θ)°. The unit-cell parameters were determined from least-squares refinements of the setting angles of 25 well centred reflections in the range θ 17–17.5°. Information concerning crystal parameters and structure refinements is summarized in Table 1. Two standard reflections monitored periodically showed no change during data collection. Intensity data were corrected for Lorentz-polarization and absorption effects.[21] The introduction of a secondary extinction coefficient was unnecessary. Of the 3539 (**3**) and 2427 (**4**) measured independent reflections, 2267 (**3**) and 2228 (**4**) were unique with $I > 3\sigma(I)$ (**3**) and $I \geqslant 3\sigma(I)$ (**4**) and used for the structure refinements.

The structures were solved by direct (**3**) and Patterson methods (**4**) followed by successive Fourier syntheses and least-squares refinements on *F* (192 parameters for complexes **3** and **4**). The computations were performed with the program CRYSTALS[22] on a MicroVax II computer. Non-hydrogen atoms were treated anisotropically. All hydrogen atoms of **3** were located on difference maps as most from **4**, the remainder in the latter being geometrically located; their positions were not refined and they were given an overall isotropic thermal parameter. Least-squares refinements with approximation to three blocks of the normal matrix were carried out by minimizing the function $\Sigma w(||F_o| - |F_c||)^2$ and each reflection was assigned a unit weight. Atomic scattering factors for neutral

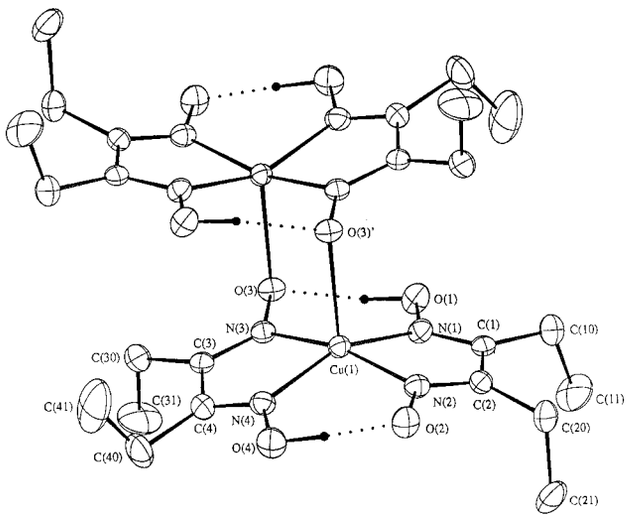

Fig. 1 Perspective view of complex **3** with the atom numbering scheme. Thermal ellipsoids are drawn at the 30% probability level. Hydrogen bonds are shown by dotted lines

Cu, O, N, C and H were taken from ref. 23. Anomalous dispersion was taken into account. Models reached convergence with R and R' indices listed in Table 1. Criteria for satisfactory complete analysis were the ratios of the root mean square (r.m.s.) shift to standard deviation being less than 0.1 and no significant features in final difference maps. The residual maxima and minima in the final Fourier-difference maps were 0.47 and −0.33 (**3**) and 1.07 and −0.61 e Å^{-3} (**4**). The molecular drawings were produced with the CAMERON[24] program. Main interatomic bond lengths and angles are listed in Tables 2 (**3**) and 3 (**4**).

Atomic coordinates, thermal parameters, and bond lengths and angles have been deposited at the Cambridge Crystallographic Data Centre (CCDC). See Instructions for Authors, *J. Chem. Soc., Dalton Trans.*, 1997, Issue 1. Any request to the CCDC for this material should quote the full literature citation and the reference number 186/301.

Results and Discussion

Structures

[{Cu(Hdeg)$_2$}$_2$] 3. The structure of complex **3** is composed of neutral centrosymmetric dinuclear [{Cu(Hdeg)$_2$}$_2$] units linked by van der Waals forces. A perspective view of the dimeric complex with the atomic numbering scheme and hydrogen bonding is depicted in Fig. 1. The two halves of the dimer are staggered so that the metal atom of one unit is directly opposite to an oxygen atom of the other. This structural feature was previously observed in the copper(II) complexes of formula [{Cu(Hdmg)$_2$}$_2$] **1**[13] and [{Cu(Hbdmg)}$_2$][ClO$_4$]$_2$ **2**.[14]

The environment of each copper atom is distorted square pyramidal, CuN$_4$O. The basal plane comprises the four oxime nitrogens from two Hdeg ligands. These four atoms are displaced 0.081 [N(1) and N(4)] below and 0.081 Å [N(2) and N(3)] above the mean basal plane. The N(1)–Cu(1)–N(2) and N(3)–Cu(1)–N(4) angles are 80.2(1) and 80.7(2)°, respectively. The four equatorial bonds to Cu(1) span a very narrow range [1.952(3)–1.966(3) Å] and are very similar to those reported for the related complexes **1** [1.946(4)–1.968(4)] and **2** [1.957(4)–1.992(5) Å]. The axial co-ordination site is occupied by the oximate oxygen atom O(3′) of the other unit. The axial bond is somewhat longer [2.263(3) Å for Cu(1)–O(3′)] than the equatorial ones and compares well with that reported for **1** [2.301(3)] and **2** [2.266(3) Å]. The copper atom is displaced by 0.336 Å toward the apex of the pyramid (0.31 and 0.297 Å in **1** and **2**, respectively). The Cu(1)N(3)O(3)Cu(1′)N(3′)O(3′) ring exhibits a chair conformation, the dihedral angle between the Cu(1)-N(3)O(3′) and N(3)O(3)N(3′)O(3′) being 52.9°. The intra-ring bond angles are 91.0(1), 122.9(2) and 106.1(2)° for O(3′)–Cu(1)–N(3), Cu(1)–N(3)–O(3) and Cu(1)–O(3′)–N(3′) (α hereafter), respectively. The value of α in **3** lies between that of **1** [102.46(22)] and **2** [107.9(3)°]. The intradimer Cu(1)···Cu(1′) distance is 3.898(1) Å (3.849 and 3.909 Å in **1** and **2**, respectively), whereas the shortest interdimer metal–metal separation [Cu(1)···Cu(1″); $-x$, $-y$, $1-z$] is 6.891(1) Å.

An oxime proton is lost from H$_2$deg in forming the complex and the resulting monoprotonated species is bound to the copper(II) ion through the oxime nitrogen atoms in a chelating fashion. The two five-membered rings at each metal ion are almost planar [largest deviation 0.043 Å at C(1) for the Cu(1)N(1)C(1)C(2)N(2) ring]. The two Cu(Hdeg)$_2$ halves adopt an umbrella shape, the magnitude of the angle between the mean planes of the two five-membered rings being 25.3°. Within the Cu(Hdeg)$_2$ moiety the remaining oxime proton in each Hdeg ligand forms a hydrogen bond with the deprotonated oximate oxygen, the oxygen–oxygen distances being 2.690(4) and 2.537(5) Å for O(3)···O(1) and O(2)···O(4), respectively [1.74 Å and 165° for O(3)···H(1) and O(1)–H(1)···O(3); 1.54 Å and 168° for O(2)···H(4) and O(4)–H(4)···O(2)]. These values are similar to the hydrogen-bonded oxygen–oxygen distances observed in the related copper(II)–oxime complexes **1**,[13] **2**,[14] [Cu$_2$(Hdmg)$_2$(H$_2$dmg)(H$_2$O)$_2$][ClO$_4$]$_2$·H$_2$O[4a] and [{Cu$_2$(dmg)(Hdmg)(H$_2$dmg)}$_2$(SO$_4$)]·2.5H$_2$O.[4b] The fact that the O(3) atom is axially bound to the Cu(1′) atom accounts for the significant lengthening of the O(3)···O(1) distance with respect to O(2)···O(4).

Table 1 Summary of crystal data* for [{Cu(Hdeg)$_2$}$_2$] **3** and [{Cu(Hchd)$_2$}$_2$] **4**

Compound	**3**	**4**
Formula	$C_{24}H_{44}Cu_2N_8O_8$	$C_{24}H_{36}Cu_2N_8O_8$
M	699.74	691.16
Crystal symmetry	Monoclinic	Triclinic
Space group	$P2_1/n$	$P\bar{1}$
a/Å	10.835(2)	8.411(1)
b/Å	17.280(5)	9.697(1)
c/Å	8.327(3)	10.018(2)
α/°		87.93(1)
β/°	95.70(3)	66.42(1)
γ/°		68.63(1)
U/Å^3	1551(2)	346(2)
Z	2	1
D_c/g cm^{-3}	1.50	1.66
F(000)	732	358
μ(Mo-Kα)/cm^{-1}	14.3	16.0
2θ Range /°	4–50	2–50
R	0.039	0.045
R'	0.043	0.049

* Details in common: $R = [\Sigma(||F_o| - |F_c||)/\Sigma|F_o|]$; $R' = [(||F_o| - |F_c||)^2/\Sigma w|F_o|^2]^{\frac{1}{2}}$.

Table 2 Selected interatomic distances (Å) and angles (°) for compound **3** with estimated standard deviations (e.s.d.s) in parentheses*

Cu(1)–N(1)	1.966(3)	Cu(1)–N(4)	1.956(3)
Cu(1)–N(2)	1.952(3)	Cu(1)–O(3′)	2.263(3)
Cu(1)–N(3)	1.955(3)		
N(1)–Cu(1)–N(2)	80.2(1)	N(2)–Cu(1)–O(3′)	104.0(1)
N(1)–Cu(1)–N(4)	155.4(1)	N(4)–Cu(1)–N(3)	80.7(2)
N(1)–Cu(1)–N(3)	96.8(1)	N(4)–Cu(1)–O(3′)	107.5(1)
N(1)–Cu(1)–O(3′)	97.0(1)	N(3)–Cu(1)–O(3′)	91.0(1)
N(2)–Cu(1)–N(4)	95.9(2)	Cu(1)–O(3′)–N(3′)	106.1(2)
N(2)–Cu(1)–N(3)	165.0(1)		

* Symmetry code: (′) $-x$, $-y$, $-z$.

Table 3 Selected interatomic distances (Å) and angles (°) for compound **4** e.s.d.s in parentheses*

Cu(1)–N(1)	1.957(4)	Cu(1)–N(4)	1.961(3)
Cu(1)–N(2)	1.936(4)	Cu(1)–O(1′)	2.242(3)
Cu(1)–N(3)	1.957(4)		
N(1)–Cu(1)–N(2)	81.2(2)	N(2)–Cu(1)–O(1′)	107.6(1)
N(1)–Cu(1)–N(3)	164.4(1)	N(3)–Cu(1)–N(4)	80.6(1)
N(1)–Cu(1)–N(4)	96.9(1)	N(3)–Cu(1)–O(1′)	101.6(1)
N(1)–Cu(1)–O(1′)	94.0(1)	N(4)–Cu(1)–O(1′)	96.2(1)
N(2)–Cu(1)–N(3)	94.8(2)	Cu(1)–O(1′)–N(1′)	106.0(2)
N(2)–Cu(1)–N(4)	156.2(2)		

* Symmetry code: (′) $-x, 1-y, -z$.

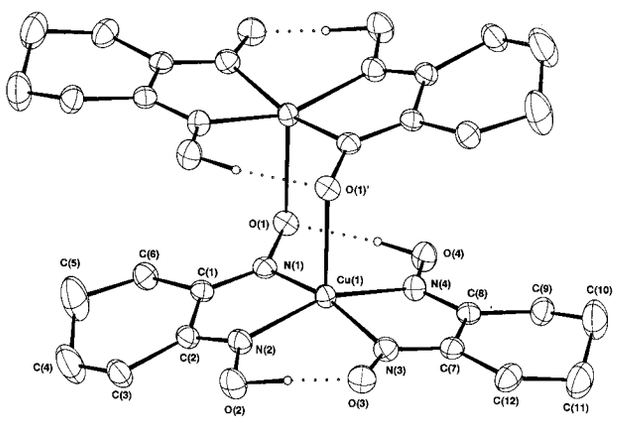

Fig. 2 Perspective view of complex **4** with the atom numbering scheme. Details as in Fig. 1

There are two types of nitrogen–oxygen bond: N(1)–O(1) and N(4)–O(4) (average 1.374 Å) and N(2)–O(2) and N(3)–O(3) (average 1.341 Å), the shorter bond distance corresponding to the deprotonated N–O (oximate) groups. This is in agreement with the greater double-bond character of the latter. The same situation is observed in the carbon–nitrogen bonds: C(1)–N(1) and C(4)–N(4) (average 1.286 Å) and C(2)–N(2) and C(3)–N(3) (average 1.303 Å).

[{Cu(Hchd)$_2$}$_2$] 4. The structure of complex **4** is made up by neutral centrosymmetric [Cu(Hchd)$_2$}$_2$] dinuclear units (Fig. 2) which are linked by van der Waals forces. As in **1**, the two Cu(Hchd)$_2$ halves are staggered in such a way that one deprotonated oxime oxygen of one half is axially bound to the copper atom of the other half.

The co-ordination environment around each copper atom can be described as a distorted square-based pyramid, CuN_4O. The four oxime nitrogens of the two Hchd ligands comprise the equatorial plane whereas the fifth co-ordination position of the square pyramid is occupied by an oximate-oxygen atom of the symmetry-related unit. The equatorial copper–oximate bond lengths lie in the range 1.936(4)–1.961(3) Å and they are very similar to that observed in **3**. The axial bond is somewhat longer [2.242(3) Å for Cu(1)–O(1′)] than the equatorial bonds but it is the shorter value in the family **1**–**4**. The largest deviation from the mean equatorial plane is 0.069 Å at N(2) and N(4) and the metal atom is pulled out from this mean plane towards the apical site by 0.334 Å. The Cu(1)N(1)O(1)Cu(1′)N(1′)O(1′) six-membered ring exhibits a chair conformation, the dihedral angle between the Cu(1)N(1)O(1) and N(1)O(1)N(1′)O(1′) planes being 51.9°. The intraring bond angles are 94.0(1), 122.9(3) and 106.0(2)° for O(1′)–Cu(1)–N(1), Cu(1)–N(1)–O(1) and Cu(1)–O(1′)–N(1′) (α), respectively. The value of α in **4** is practically identical to that of **3**. The intradimer Cu(1)···Cu(1′) distance is 3.825(1) Å, whereas the shortest interdimer metal–metal separation [Cu(1)···Cu(1″), $1-x, 1-y, 1-z$] is 6.502(1) Å.

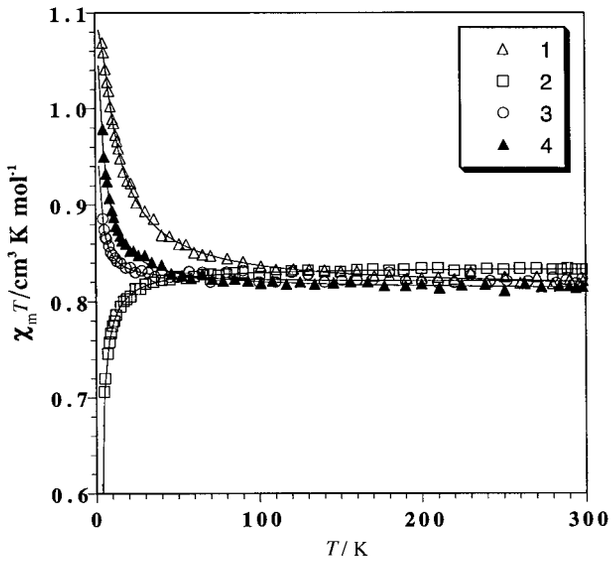

Fig. 3 Thermal dependence of the product $\chi_m T$ [χ_m being the magnetic susceptibility per two copper(II) ions] for complexes **1**–**4**: (Δ, □, O, ▲) experimental points; (—) best theoretical fit (see text)

Two monodeprotonated Hchd$^-$ ligands co-ordinate to the copper(II) ion in a chelating fashion through the oxime nitrogen atoms forming two five-membered chelate rings which are planar [largest deviation 0.047 Å at N(1) for Cu(1)N(1)C(1)C(2)N(2) and 0.045 Å at N(3) for Cu(1)N(3)C(7)C(8)N(4)]. As in **3**, the two Cu(Hchd)$_2$ units adopt an umbrella shape, the dihedral angle between the mean planes of the two five-membered rings being 25.7°. The H(2) and H(4) oxime protons which are attached to oxygens O(1) and O(3) are involved in strong hydrogen bonds with the ionized O(2) and O(4) oxime atoms: the O(1)···O(4) and O(2)···O(3) separations are 2.724(4) and 2.545(5) Å, respectively [1.78 Å and 164° for O(1)···H(4) and O(4)–H(4)···O(1); 1.43 Å and 165° for O(3)···H(2) and O(2)–H(2)···O(3)]. As in **3**, the significant lengthening of the O(1)···O(4) distance is most likely due to the weak axial co-ordination of O(1).

Magnetic properties

The temperature dependence of the product $\chi_m T$ for complexes **1**–**4** is shown in Fig. 3. The value of $\chi_m T$ at room temperature for these complexes is about 0.83 cm^3 K mol^{-1}, consistent with the occurrence of two non-interacting copper(II) ions; it slightly decreases (**2**) or increases (**1**, **3** and **4**) when cooling and reaches a value of 1.07 (**1**), 0.70 (**2**), 0.89 (**3**) and 0.98 cm^3 K mol^{-1} (**4**) at 4.2 K. In the case of complex **2**, no maximum is observed in the susceptibility curve in the investigated temperature range. These features reflect the occurrence of weak intramolecular antiferro- (**2**) and ferro-magnetic interactions (**1**, **3** and **4**). Given the dimeric structure of these compounds, we have analysed their magnetic behaviour through a simple Bleaney–Bowers expression for two local doublets [equation (1)], where J is the singlet–triplet energy gap, g the average g

$$\chi_m T = (2N\beta^2 g^2/k)[3 + \exp(-J/kT)]^{-1} \qquad (1)$$

factor and N, β and k have their usual meanings. Least-squares fitting of the experimental data led to $J = +9.1$ cm^{-1}, $g = 2.10$ and $R = 3.1 \times 10^{-5}$ for **1**, $J = -1.9$ cm^{-1}, $g = 2.11$ and $R = 9.8 \times 10^{-5}$ for **2**, $J = +1.0$ cm^{-1}, $g = 2.09$ and $R = 2.1 \times 10^{-4}$ for **3** and $J = +3.1$ cm^{-1}, $g = 2.12$ and $R = 1.1 \times 10^{-4}$ for **4**,

Table 4 Selected magnetostructural data for complexes **1–4**

Compound	d_{Cu-N}[a]/Å	R_{ax}[b]/Å	α/°	$d_{Cu\cdots Cu}$[c]/Å	J/cm^{-1}
1	1.953	2.301(3)	102.46(22)	3.849	+9.1
2	1.976	2.266(3)	107.9(3)	3.909	−1.9
3	1.957	2.263(3)	106.1(2)	3.898(1)	+1.0
4	1.940	2.242(3)	106.0(2)	3.825(1)	+3.1

[a] Average value for the copper to the oxime-nitrogen bond. [b] Distance from the copper to the oxime-oxygen atom. [c] Intramolecular metal–metal separation.

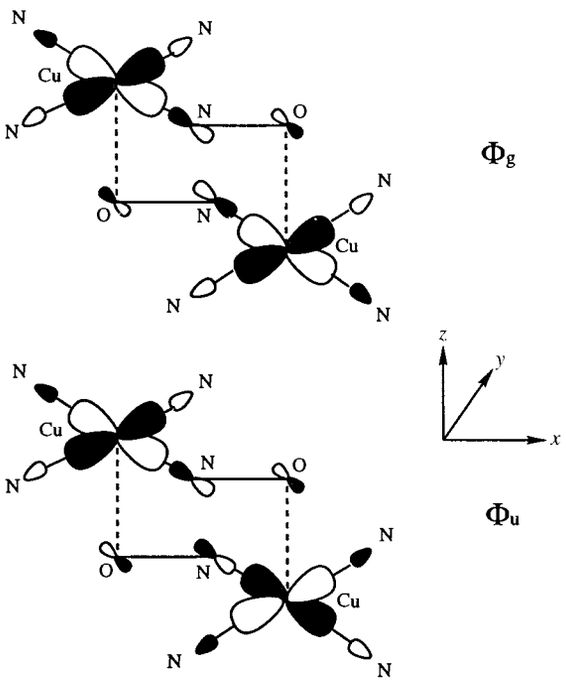

Scheme 2

where R is the agreement factor defined as $\Sigma_i[(\chi_m T)_{obs}(i) - (\chi_m T)_{calc}(i)]^2/\Sigma_i[(\chi_m T)_{obs}(i)]^2$. The low-lying triplet state for complex **1** was observed for the first time by Villa and Hatfield[15] through variable-temperature solid-state EPR and magnetic studies. Their analysis of the preliminary magnetic susceptibility data led to values of +29 cm^{-1}, 2.157 and −1.45 K for J, g and θ (Weiss constant), respectively. Our study reveals that a very good fit of the magnetic data is obtained without intermolecular interactions (that is θ = 0), the value of J for **1** also being positive but significantly smaller.

Two main points deserve consideration in this family of related copper(II) dimers: (*i*) the exchange pathway through the out-of-plane oximato bridge and (*ii*) the structural factors which are responsible for this change from ferromagnetic (**1**, **3** and **4**) to antiferromagnetic coupling (**2**). A comparison of the structures of **1–4** reveals that the four short metal to ligand bonds are the Cu–N (oxime) bonds and their average values are very similar in this series (see Table 4). Consequently, the magnetic orbital describing the unpaired electron on each mononuclear fragment corresponds to a d_{xy} type orbital which is partially delocalized through the oximato bridge (see Scheme 2). The weaker magnetic coupling in these oximato-bridged complexes exhibiting an out-of-plane topology with respect to the stronger one observed in that with an in-plane topology can be easily understood by comparing Schemes 1 and 2: the highest occupied molecular orbitals (HOMOs) in the oxime groups in Scheme 1 are better adapted to delocalize the spin density than that in Scheme 2.

The most significant structural differences are the value of

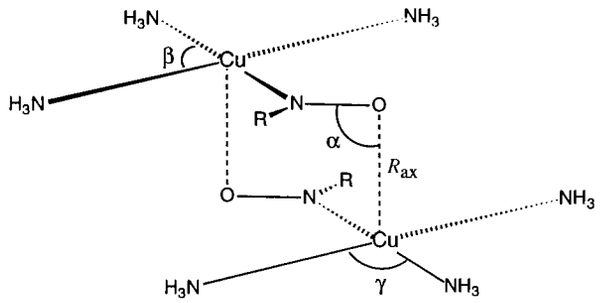

Scheme 3 R = CH_2

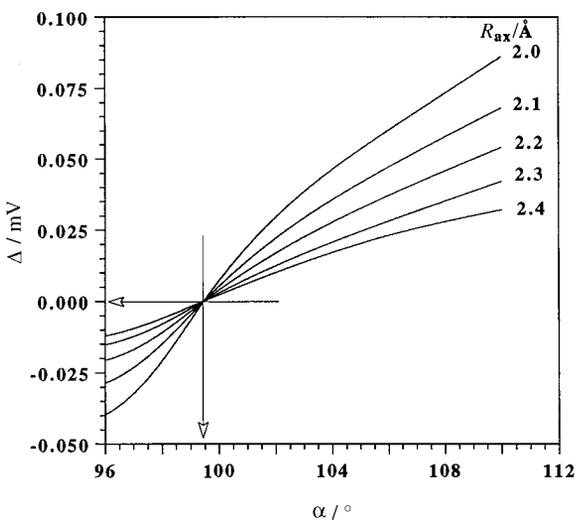

Fig. 4 Plot of the variation of Δ against α for different values of the Cu–O (axial) distance (R_{ax}) in the model system in Scheme 3. Average bond distances and angles from complexes **1–4** were used in the calculations

the axial Cu–O (oxime) bond length (R_{ax}) and that of the angle α (see Table 4). A semiquantitative interpretation of the influence of both parameters on the magnetic behaviour of complexes **1–4** can be obtained in the framework of localized orthogonal magnetic orbitals a and b[25] as proposed by Hay *et al.*[26] For symmetrical complexes, it is found that the singlet–triplet energy gap is given by expression (2) where Δ is the energy gap between

$$J = 2K_{ab} - [\Delta^2/(J_{aa} - J_{ab})] \quad (2)$$

the singly occupied molecular orbitals Φ_g and Φ_u (see Scheme 2), K_{ab} is the two-electron exchange integral between a and b, and J_{aa} and J_{ab} are the two-electron Coulomb integrals defined by Hay *et al.*[26] The first term is always positive (ferromagnetic component) and the second is negative (antiferromagnetic component). In a series of complexes of similar geometries as is in the present case the two-electron integrals are assumed to be constant. Consequently, the value of Δ^2 can be used to follow the evolution of J in the family of complexes **1–4**. Extended-Hückel calculations allow one to evaluate Δ. The results of these calculations on the dimer model shown in Scheme 3* obtained by using the CACAO program[27] are shown in Fig. 4. It can be seen that R_{ax} has a small influence on the value of Δ in contrast to the greater influence of α in this family. So, changes in the value of R_{ax} between 2.24 and 2.30 Å result in an increase of the value of Δ of less than 15%, whereas its value increases by *ca.* 60% when α goes from 102.5 to 108°. In this respect, the key

* Average values for the Cu–N (1.960), N–O (1.350) and N–C (1.28 Å) bond distances for the β (100) and γ (80°) bond angles were used. The ideal value (120°) was kept for the O–N–Cu and C–N–Cu bonds. The atomic parameters in the Hückel calculations were taken from ref. 5(*b*).

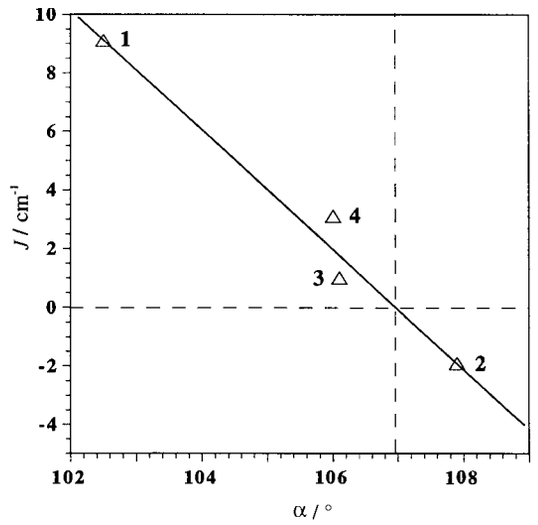

Fig. 5 Plot of the singlet–triplet energy gap (J) against α for complexes **1**–**4**

point is that the variation of Δ as a function of α is essentially tuned by the out-of-plane overlap between the d_{xy}-type orbital of one mononuclear fragment and the HOMO of the axial oxime group. For α = 99.5°, Φ_g and Φ_u are degenerate and Δ = 0. At this point the ferromagnetic coupling would attain its maximum value. When α is increased the orbital interaction becomes antibonding in Φ_g and bonding in Φ_u causing an increase in Δ and thus leading to a progressive stabilization of the singlet state. A plot of the variation of J against α for the present series (Fig. 5) shows a quasi-linear correlation. The ferro- and antiferro-magnetic terms cancel each other for α *ca.* 106.9°, the ground state being a triplet for α < 106.9° and a singlet for α > 106.9°.

In order to check the validity of the present correlation, it is clear that the range of values of α, which at the present moment is very limited, has to be increased. At first sight this is not a difficult task because of the great number of alkyl substituents which can be attached to the imine-carbon atoms. However, special attention should be paid to their size because of the occurrence of steric hindrance between the substituents of the two monomeric fragments in the resulting dimer. In fact, they could preclude the dimeric arrangement observed in the complexes **1**–**4**. This is the case for the mononuclear compound of formula $[Cu(H_2O)(Hdpg)_2]$[28] (H_2dpg = diphenylglyoxime), where two monodeprotonated diphenylglyoximate ligands and a co-ordinated water molecule comprise a square-pyramidal environment around the copper atom, the water molecule occupying the axial position.

Acknowledgements

Financial support from the Dirección General de Investigación Científica y Técnica (DGICYT, Spain) through Project PB94-1002, the Spanish–French Integrated Actions, the Human Capital and Mobility Program (Network on Magnetic Molecular Materials from EEC) through grant ERBCHXCT920080 and the State Committee for Scientific Research (Warsaw, Poland) through Project 3T09A06308 is gratefully acknowledged. Three of us are indebted to the Consellería de Cultura, Educació i Ciència de la Generalitat Valenciana (B. C. and R. R.) and to the Ministerio de Educación y Ciencia (J. C.) for pre- and post-doctoral grants.

References

1 G. Mohanty, S. Baral, R. P. Singh and A. Chakravorty, *J. Inorg. Nucl. Chem. Lett.*, 1974, **10**, 665.
2 J. A. Bertrand, J. H. Smith and P. G. Eller, *Inorg. Chem.*, 1974, **13**, 1649; J. A. Bertrand, J. H. Smith and D. G. Van Derveer, *Inorg. Chem.*, 1977, **16**, 1477.
3 D. Luneau, H. Oshio, H. Okawa, M. Koikawa and S. Kida, *Bull. Chem. Soc. Jpn.*, 1990, **63**, 2212.
4 (*a*) R. Ruiz, J. Sanz, B. Cervera, F. Lloret, M. Julve, C. Bois, J. Faus and M. C. Muñoz, *J. Chem. Soc., Dalton Trans.*, 1993, 1623; (*b*) R. Ruiz, J. Sanz, F. Lloret, M. Julve, J. Faus, C. Bois and M. C. Muñoz, *J. Chem. Soc., Dalton Trans.*, 1993, 3035; (*c*) R. Ruiz, F. Lloret, M. Julve, M. C. Muñoz and C. Bois, *Inorg. Chim. Acta*, 1994, **219**, 179.
5 (*a*) M. Julve, M. Verdaguer, O. Kahn, A. Gleizes and M. Philoche-Levisalles, *Inorg. Chem.*, 1984, **23**, 3808; (*b*) S. Alvarez, M. Julve and M. Verdaguer, *Inorg. Chem.*, 1990, **29**, 4501.
6 M. Verdaguer, O. Kahn, M. Julve and A. Gleizes, *Nouv. J. Chim.*, 1985, **9**, 325; Y. Journaux, J. Sletten and O. Kahn, *Inorg. Chem.*, 1985, **24**, 4063; A. Bencini, C. Benelli, A. C. Fabretti, G. Franchini and D. Gatteschi, *Inorg. Chem.*, 1986, **25**, 1063; H. Okawa, N. Matsumoto, M. Koikawa, K. Takeda and S. Kida, *J. Chem. Soc., Dalton Trans.*, 1990, 1383; J. L. Sanz, B. Cervera, R. Ruiz, C. Bois, J. Faus, F. Lloret and M. Julve, *J. Chem. Soc., Dalton Trans.*, 1996, 1359 and refs. therein.
7 R. Veit, J. J. Girerd, O. Kahn, F. Robert and Y. Jeannin, *Inorg. Chem.*, 1986, **25**, 4175.
8 R. Vicente, J. Ribas, S. Alvarez, A. Seguí and M. Verdaguer, *Inorg. Chem.*, 1987, **26**, 4004.
9 (*a*) Z. J. Zhong, H. Okawa, N. Matsumoto, H. Sakiyama and S. Kida, *J. Chem. Soc., Dalton Trans.*, 1991, 497; (*b*) R. Ruiz, F. Lloret, M. Julve, J. Faus, M. C. Muñoz and X. Solans, *Inorg. Chim. Acta*, 1993, **213**, 261; (*c*) F. Birkelbach, M. Winter, U. Flörke, H. J. Haupt, C. Butzlaff, M. Lengen, E. Bill, A. X. Trautwein, K. Wieghardt and P. Chaudhuri, *Inorg. Chem.*, 1994, **33**, 3990; (*d*) E. Colacio, J. M. Domínguez-Vera, A. Escuer, R. Kivekas and A. Romerosa, *J. Chem. Soc., Dalton Trans.*, 1994, 3914; (*e*) D. Burdinski, F. Birkelbach, M. Gerdan, A. X. Trautwein, K. Wieghardt and P. Chaudhuri, *J. Chem. Soc., Chem. Commun.*, 1995, 963.
10 H. Okawa, M. Koikawa, S. Kida, D. Luneau and H. Oshio, *J. Chem. Soc., Dalton Trans.*, 1990, 469; D. Luneau, H. Oshio, H. Okawa and S. Kida, *J. Chem. Soc., Dalton Trans.*, 1990, 2283; P. Chaudhuri, M. Winter, P. Fleischhauer, W. Haase, U. Flörke and H. J. Haupt, *J. Chem. Soc., Chem. Commun.*, 1990, 1728; P. Chaudhuri, M. Winter, B. P. C. Della Védova, E. Bill, A. Trautwein, S. Gehring, P. Fleischhauer, B. Nuber and J. Weiss, *Inorg. Chem.*, 1991, **30**, 2148; P. Chaudhuri, M. Winter, F. Birkenbach, P. Fleischhauer, W. Haase, U. Flörke and H. J. Haupt, *Inorg. Chem.*, 1991, **30**, 4293; P. Chaudhuri, M. Winter, B. P. C. Della Védova, P. Fleischhauer, W. Haase, U. Flörke and H. J. Haupt, *Inorg. Chem.*, 1991, **30**, 4777.
11 P. Chaudhuri, M. Winter, P. Fleischhauer, W. Haase, U. Flörke and H. J. Haupt, *J. Chem. Soc., Chem. Commun.*, 1993, 566; *Inorg. Chim. Acta*, 1993, **212**, 241; P. Chaudhuri, F. Birkelbach, M. Winter, V. Staemmler, P. Fleischhauer, W. Haase, U. Flörke and H. J. Haupt, *J. Chem. Soc., Dalton Trans.*, 1994, 2313; C. Krebs, M. Winter, T. Weyhermüller, E. Bill, K. Wieghardt and P. Chaudhuri, *J. Chem. Soc., Chem. Commun.*, 1995, 1913.
12 (*a*) F. Lloret, R. Ruiz, M. Julve, J. Faus, Y. Journaux, I. Castro and M. Verdaguer, *Chem. Mater.*, 1992, **4**, 1150; (*b*) F. Lloret, R. Ruiz, B. Cervera, I. Castro, M. Julve, J. Faus, J. A. Real, F. Sapiña, Y. Journaux, J. C. Colin and M. Verdaguer, *J. Chem. Soc., Chem. Commun.*, 1994, 2615.
13 (*a*) E. Frasson, R. Bardi and S. Brezzi, *Acta Crystallogr.*, 1959, **12**, 201; (*b*) A. Vaciago and L. Zambonelli, *J. Chem. Soc. A*, 1970, 218.
14 Y. M. Wang, C. C. Wang, S. L. Wang and C. S. Chung, *Acta Crystallogr., Sect. C*, 1990, **46**, 1770.
15 J. F. Villa and W. E. Hatfield, *J. Chem. Phys.*, 1971, **55**, 4758.
16 G. Brauer, *Handbook of Preparative Inorganic Chemistry*, Academic Press, New York and London, 1963, vol. 2, p. 1013.
17 R. Blinc and D. Hadzi, *J. Chem. Soc.*, 1958, 4536; J. Caton and C. V. Banks, *Inorg. Chem.*, 1967, **6**, 1670; D. H. Svedung, *Acta Chem. Scand.*, 1969, **23**, 2865; J. Bassett, J. Bensted and R. Grzekowiak, *J. Chem. Soc. A*, 1969, 2873.
18 A. Bigotto, G. Costa, V. Galasso and G. De Alti, *Spectrochim. Acta, Part A*, 1970, **26**, 1939; A. Bigotto, V. Galasso and G. De Alti, *Spectrochim. Acta, Part A*, 1971, **27**, 1659.
19 J. C. Bernier and P. Poix, *Actual. Chim.*, 1978, **2**, 7.
20 A. Earnshaw, *Introduction to Magnetochemistry*, Academic Press, London, New York, 1968.
21 N. Walker and D. Stuart, *Acta Crystallogr.*, 1983, **39**, 158.
22 D. J. Watkins, J. R. Carruthers and P. W. Betteridge, CRYSTALS, An advanced crystallographic computer program system, Chemical Crystallographic Laboratory, University of Oxford, 1988.

23 *International Tables for X-Ray Crystallography*, Kynoch Press, Birmingham, 1974, vol. 4.
24 L. J. Pearce and D. J. Watkins, CAMERON, Crystallography Laboratory, Oxford, 1992.
25 J. J. Girerd, Y. Journaux and O. Kahn, *Chem. Phys. Lett.*, 1981, **82**, 534.
26 P. J. Hay, J. C. Thibeault and R. Hoffmann, *J. Am Chem. Soc.*, 1975, **97**, 4884.
27 C. Mealli and D. M. Proserpio, CACAO, Computer Aided Composition of Atomic Orbitals, PC Version, 1992; see *J. Chem. Educ.*, 1990, **67**, 399.
28 M. Boualan and A. Gleizes, *Z. Kristallogr.*, 1983, **164**, 141.

Received 25*th June* 1996; *Paper* 6/04420D